

A Gaussian-2 and Gaussian-3 Study of Alkoxide Anion Decompositions. 1. H₂ and CH₄ Eliminations of the Methoxide, Ethoxide, Isopropoxide, and *tert*-Butoxide Anions

S.-W. Chiu*

Beckman Institute, University of Illinois, 405 N. Mathews Avenue, Urbana, Illinois 61801

Justin Kai-Chi Lau and Wai-Kee Li*

Department of Chemistry, The Chinese University of Hong Kong, Shatin, N.T., Hong Kong

Received: May 31, 2000; In Final Form: September 20, 2000

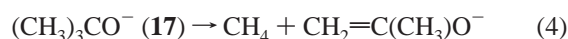
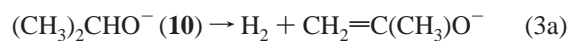
The decomposition mechanisms of four alkoxide anions, CH₃O⁻, CH₃CH₂O⁻, (CH₃)₂CHO⁻, and (CH₃)₃CO⁻, have been studied with modified G2 (G2++) and G3 methods. The energy profiles for the decomposition reactions of each alkoxide anion are reported. It is found that the decompositions proceed via an anionic mechanism with a stepwise pathway. For anions CH₃CH₂O⁻ and (CH₃)₂CHO⁻, calculated results indicate that the H₂ elimination has a lower energy barrier than the CH₄ elimination. This result is in total agreement with the experimental data obtained in the collision-activated dissociation and infrared multiple photon induced elimination studies of simple alkoxide anions.

Introduction

There have been various interests in alkoxide anions (RO⁻) in the gas phase.^{1–12} The gas-phase acidities of a large number of alcohols have been determined from studies of the unimolecular collision-activated dissociation (CAD) of proton-bound cluster ions [RO⋯H⋯OR']⁻.¹ Extensive CAD studies of simple and complex alkoxides have been reported.^{2–8} From ab initio calculations and a study of isotope effects, Bowie and co-workers^{9,10} have investigated the mechanism of elimination reactions of ethoxide and *tert*-butoxide. They pointed out that the two reactions should be similar and have a stepwise mechanism. The technique of infrared multiple photon (IRMP) photochemistry has also been applied to study the mechanism of decomposition of alkoxides.^{11,12} Tumas et al. have studied the decompositions of 15 alkoxide anions. They reported that the decomposition should start with a heterolytic cleavage rather than a homolytic one. The charge inversion mass spectra of alkoxides have been reported.¹³ Recently, a high-level theoretical study of intramolecular rearrangements and unimolecular fragmentation of ethoxide has been described.¹⁴ Structures, charge distributions,^{15,16} and fundamental vibrational frequencies¹⁵ of selected alkoxides have also been investigated theoretically.

Loss of H₂ or CH₄ from primary alkoxide anions proceeds via a stepwise 1,2-elimination pathway involving ion–molecular complexes (IMCs)¹⁷ as intermediates.^{9–12} Secondary alkoxide anions, unlike the primary ones, can have more than one fragmentation pathway. Isopropoxide, for example, can in principle undergo both H₂ and CH₄ eliminations.^{2,9} As noted by Mercer and Harrison,² Bowie et al.⁹ also reported that CD₃H was eliminated from (CD₃)₂CHO⁻, a result which is inconsistent with the proposed 1,2-elimination reaction. The observed products CH₃D and CD₃H, as listed in Table 1 of ref 9, would probably be due to 1,1-elimination reactions of (CH₃)₂CDO⁻ and (CD₃)₂CHO⁻, respectively.

In this work, we undertake the study of the following plausible 1,1- and 1,2-elimination reactions of CH₃O⁻, CH₃CH₂O⁻, (CH₃)₂CHO⁻, and (CH₃)₃CO⁻ at a high theoretical level:



Such a study would lead to a better understanding of the energetics of the fragmentations of these simple alkoxide anions. In addition, there have been questions raised regarding the alkoxide anion decomposition reactions: (1) Do they proceed via a stepwise or a concerted mechanism? (2) Why is the heterolytic cleavage more favorable than the homolytic one? (3) Why does CH₃CH₂O⁻ undergo H₂ elimination exclusively, as observed experimentally?¹² (4) Does (CH₃)₂CHO⁻ undergo 1,2-eliminations of H₂ and CH₄, as well as 1,1-elimination of CH₄?^{2,7,9,12} We will attempt to answer these questions in this work.

Methods of Calculations

All calculations were carried out on DEC 500au and SGI10000 workstations, as well as on an SGI Origin 2000 High-Performance Server, using the Gaussian 94¹⁸ and Gaussian 98¹⁹ packages of programs. The computational models we employed were the modified Gaussian-2 (G2++)¹⁴ and Gaussian-3 (G3)²⁰ levels of theory. In the G3 model, structures are optimized at the second-order Møller–Plesset theory (MP2) using the 6-31G(d) basis set with all electrons included, i.e., at the MP2(Full)/6-31G(d) level. For some species, diffuse functions were added for optimization, i.e., at the MP2(Full)/6-31++G(d)

TABLE 1: Heterolytic and Homolytic Bond Dissociation Energies of Various Alkoxide Anions at the G3 Level^a

| | | | | |
|--|---|--|---|---|
| H ₂ C=O + H ⁻ | ← | CH ₃ O ⁻ (1) | → | H ₂ C=O ⁻ + H [•] |
| 182.1 | | 0 | | 313.2 |
| (CH ₃)HC=O + H ⁻ | ← | CH ₃ CH ₂ O ⁻ (4) | → | (CH ₃)HC=O ⁻ + H [•] |
| 176.8 | | 0 | | 322.1 |
| H ₂ C=O + CH ₃ ⁻ | ← | CH ₃ CH ₂ O ⁻ (4) | → | H ₂ C=O ⁻ + [•] CH ₃ |
| 206.0 | | 0 | | 287.0 |
| (CH ₃) ₂ C=O + H ⁻ | ← | (CH ₃) ₂ CHO ⁻ (10) | → | (CH ₃) ₂ C=O ⁻ + H [•] |
| 175.8 | | 0 | | 319.9 |
| (CH ₃)HC=O + CH ₃ ⁻ | ← | (CH ₃) ₂ CHO ⁻ (10) | → | (CH ₃)HC=O ⁻ + [•] CH ₃ |
| 201.4 | | 0 | | 296.7 |
| (CH ₃) ₂ C=O + CH ₃ ⁻ | ← | (CH ₃) ₂ CO ⁻ (17) | → | (CH ₃) ₂ C=O ⁻ + [•] CH ₃ |
| 195.5 | | 0 | | 289.5 |

^a The species shown in the first column are the products of a heterolytic cleavage of the alkoxide anions given in the middle column; those given in the last column are the products of a homolytic cleavage.

level, to obtain a more reasonable geometry. Based on these optimized structures, single-point calculations at QCISD(T)/6-31G(d), MP4/6-31G(d), MP4/6-31+G(d), MP4/6-31G(2df,p), and MP2(Full)/G3large levels are required for the G3 model. Also, this model requires higher level correction (HLC) in the calculation of total electronic energies (E_e). The MP2(Full)/6-31G(d) or MP2(Full)/6-31++G(d) harmonic vibrational frequencies, scaled by 0.9661 and 0.972, respectively, are applied for the zero-point vibrational energy (ZPVE) correction at 0 K ($E_0 = E_e + \text{ZPVE}$).

In the G2++ model,¹⁴ all the structures are optimized at MP2(Full)/6-31++G(d) level with diffuse functions included on both heavy and hydrogen atoms. In the energy calculations, some modifications have been made on the original G2²¹ single points: QCISD(T)/6-311G(d,p), MP4/6-311G(d,p), MP4/6-311++G(d,p) [with additional diffuse functions for hydrogen atom], MP4/6-311G(2df,p), and MP2/6-311++(3df,2p) [with additional diffuse functions for hydrogen atom]. HLC is added to account for the remaining basis set deficiencies: $\text{HLC} = -Bn_\beta - An_\alpha$, where $A = 0.18$, $B = 5.03$ mhartrees (mh), n_α and n_β are the number of α and β valence electrons, respectively, and $n_\alpha \geq n_\beta$. All the structures have been characterized by vibrational frequency calculations at the MP2(Full)/6-31++G(d) level with scaling factor (0.972) applied for the ZPVE corrections.

The G2++/G3 heats of formation at temperature T ($\Delta H_f^\circ(T)$) in this work were calculated in the following manner. For molecule AB, its G2++/G3 $\Delta H_f^\circ(T)$ was calculated from the G2++/G3 heat of reaction $\Delta H_r^\circ(T)(A+B \rightarrow AB)$ and the respective experimental $\Delta H_f^\circ(T)(A)$ and $\Delta H_f^\circ(T)(B)$ for elements A and B. In the calculations of $\Delta H_f^\circ(T)$ for anions, we set the $\Delta H_f^\circ(T)$ value of a free electron to be zero.

In this work, many transition structures (TSs) were located. For each TS, the “reactant(s)” and “product(s)” were confirmed by intrinsic reaction coordinate calculations.

Results and Discussion

In our notation, single- or double-digit numerals such as **1** and **2**, etc. refer to stable alkoxide anion structures, fragmentation intermediates, or fragments. In addition, the transition structure connecting **1** and **2** is denoted as TS(**1**→**2**), etc.

The bond dissociation energies for the homolytic versus heterolytic bond cleavage of the four alkoxide anions studied in this work, namely, the methoxide (**1**), ethoxide (**4**), isopropoxide (**10**), and *tert*-butoxide (**17**) anions, are listed in Table 1. The G2++ and G3 results for reactions 1–4 are summarized in Tables 2–5, respectively; also, the energy profiles of the same

TABLE 2: G2++ and G3 Total Energies^a (E_0), Enthalpies (H_{298}), and Standard Heats of Formation at 0 K ($\Delta H_f^\circ(0)$) and 298 K ($\Delta H_f^\circ(298)$) of the Species Involved in the Fragmentation Reaction of CH₃O⁻

| species | E_0 (hartrees) | H_{298} (hartrees) | $\Delta H_f^\circ(0)$ (kJ mol ⁻¹) | $\Delta H_f^\circ(298)$ (kJ mol ⁻¹) |
|---------------------------|---------------------|-------------------------|--|--|
| 1 | -114.929 09 | -114.925 22 | -132.5 | -139.5 |
| | <i>-115.018 83</i> | <i>-115.014 99</i> | <i>-119.3</i> | <i>-126.3</i> |
| | | | | (-139 ± 10) ^b |
| | | | | (-134 ± 4.6) ^c |
| 2 | -114.879 84 | -114.874 15 | -3.2 | -5.4 |
| | <i>-114.968 53</i> | <i>-114.963 58</i> | <i>12.8</i> | <i>8.7</i> |
| 3a + 3b | -114.879 94 | -114.872 83 | | |
| | <i>-114.969 72</i> | <i>-114.962 61</i> | | |
| TS(1 → 2) | -114.882 71 | -114.878 25 | -10.8 | -16.1 |
| | <i>-114.969 32</i> | <i>-114.964 83</i> | <i>10.7</i> | <i>5.4</i> |
| TS(2 → 3) | -114.868 22 | -114.863 40 | 27.3 | 22.9 |
| | <i>-114.958 62</i> | <i>-114.953 56</i> | <i>38.8</i> | <i>35.0</i> |

^a G2++ energies are shown in bold font, and G3 energies are in italic font. ^b Experimental value, taken from ref 43, is given in parentheses. ^c Experimental value, taken from ref 44, is given in parentheses.

TABLE 3: G2++ and G3 Total Energies^a (E_0), Enthalpies (H_{298}), and Standard Heats of Formation at 0 K ($\Delta H_f^\circ(0)$) and 298 K ($\Delta H_f^\circ(298)$) of the Species Involved in the Fragmentation Reaction of CH₃CH₂O⁻

| species | E_0 (hartrees) | H_{298} (hartrees) | $\Delta H_f^\circ(0)$ (kJ mol ⁻¹) | $\Delta H_f^\circ(298)$ (kJ mol ⁻¹) |
|---------------------------|---------------------|-------------------------|--|--|
| 4 | -154.164 26 | -154.159 45 | -172.6 | -186.1 |
| | <i>-154.299 30</i> | <i>-154.294 56</i> | <i>-159.5</i> | <i>-173.2</i> |
| | | | | (-186 ± 10) ^b |
| | | | | (-183 ± 9) ^c |
| 5 | -154.117 22 | -154.110 49 | -49.1 | -57.6 |
| | <i>-154.252 49</i> | <i>-154.245 80</i> | <i>-36.6</i> | <i>-45.2</i> |
| 6 | -154.120 21 | -154.113 62 | -56.9 | -65.8 |
| | <i>-154.253 22</i> | <i>-154.246 73</i> | <i>-38.5</i> | <i>-47.7</i> |
| 7a + 7b | -154.161 31 | -154.152 74 | | |
| | <i>-154.297 10</i> | <i>-154.289 24</i> | | |
| 8 | -154.105 11 | -154.097 00 | -17.3 | -22.2 |
| | <i>-154.239 32</i> | <i>-154.231 88</i> | <i>-2.0</i> | <i>-8.7</i> |
| 9a + 9b | -154.123 62 | -154.116 00 | | |
| | <i>-154.258 34</i> | <i>-154.250 73</i> | | |
| TS(4 → 5) | -154.116 27 | -154.110 80 | -46.6 | -58.4 |
| | <i>-154.252 55</i> | <i>-154.247 13</i> | <i>-36.8</i> | <i>-48.7</i> |
| TS(5 → 6) | -154.117 50 | -154.111 54 | -49.8 | -60.4 |
| | <i>-154.252 75</i> | <i>-154.246 82</i> | <i>-37.3</i> | <i>-47.9</i> |
| TS(6 → 7) | -154.119 05 | -154.113 65 | -53.9 | -65.9 |
| | <i>-154.255 79</i> | <i>-154.250 44</i> | <i>-45.3</i> | <i>-57.4</i> |
| TS(4 → 8) | -154.105 42 | -154.097 82 | -18.1 | -24.3 |
| | <i>-154.239 45</i> | <i>-154.232 51</i> | <i>-2.4</i> | <i>-10.3</i> |
| TS(8 → 9) | -154.099 81 | -154.092 70 | -3.4 | -10.9 |
| | <i>-154.235 20</i> | <i>-154.228 18</i> | <i>8.8</i> | <i>1.0</i> |

^a G2++ energies are shown in bold font, and G3 energies are in italic font. ^b Experimental value, taken from ref 43, is given in parentheses. ^c Experimental value, taken from ref 44, is given in parentheses.

reactions are schematically shown in Figures 1–4, respectively. The geometries of all the equilibrium and transition structures involved in these reactions are depicted in Figure 5. Throughout this work, G2++ energies are used for discussion unless explicitly stated otherwise.

Nature of Ion–Neutral Complex. In general, the unimolecular decomposition of a variety of gaseous ions is mediated by ion–neutral complexes (INCs).^{11,22–28} In this mechanism, a covalent bond cleaves in such a fashion that the charged and neutral fragments are held together by electrostatic interaction and the fragments sojourn in the vicinity of one another long enough to undergo a subsequent ion–neutral reaction.²² Such an INC may not necessarily correspond to a local potential energy minimum.²⁹ The internal rotational degrees of freedom

TABLE 4: G2++ and G3 Total Energies^a (E_0), Enthalpies (H_{298}), and Standard Heats of Formation at 0 K (ΔH_f°) and 298 K (ΔH_f°) of the Species Involved in the Fragmentation Reaction of $(\text{CH}_3)_2\text{CHO}^-$

| species | E_0 (hartrees) | H_{298} (hartrees) | ΔH_f° (kJ mol ⁻¹) | ΔH_f° (kJ mol ⁻¹) |
|------------------------------|---------------------|-------------------------|---|---|
| 10 | -193.399 36 | -193.393 33 | -212.5 | -231.9 |
| | -193.580 06 | -193.574 08 | -200.5 | -220.1 |
| | | | | (-232 ± 10) ^b |
| | | | | (-231 ± 9) ^c |
| 11 | -193.357 94 | -193.350 30 | -103.7 | -118.9 |
| | -193.537 51 | -193.530 78 | -88.8 | -106.4 |
| 12a + 12b | -193.393 38 | -193.384 08 | | |
| | -193.574 28 | -193.565 21 | | |
| 13 | -193.343 18 | -193.334 12 | -65.0 | -76.4 |
| | -193.521 79 | -193.512 61 | -47.5 | -58.7 |
| 14a + 14b | -193.364 95 | -193.356 14 | | |
| | -193.542 81 | -193.533 90 | | |
| 15 | -193.343 18 | -193.334 13 | -64.8 | -76.6 |
| | -193.521 79 | -193.512 61 | -47.5 | -58.7 |
| 16a + 16b | -193.404 97 | -193.395 89 | | |
| | -193.585 72 | -193.577 36 | | |
| TS(10→11) | -193.350 68 | -193.343 98 | -84.6 | -102.3 |
| | -193.529 30 | -193.522 65 | -67.2 | -85.1 |
| TS(11→12) | -193.355 95 | -193.349 20 | -98.5 | -116.0 |
| | -193.536 59 | -193.530 41 | -86.4 | -105.4 |
| TS(10→13) | -193.342 68 | -193.334 93 | -63.7 | -78.6 |
| | -193.521 14 | -193.513 04 | -45.8 | -59.8 |
| TS(13→14) | -193.335 72 | -193.326 91 | -45.4 | -57.5 |
| | -193.515 27 | -193.506 80 | -30.4 | -43.4 |
| TS(10→15) | -193.342 69 | -193.334 94 | -63.5 | -78.7 |
| | -193.521 11 | -193.513 02 | -45.7 | -59.8 |
| TS₁(15→16) | -193.342 88 | -193.334 69 | -64.0 | -78.0 |
| | -193.521 11 | -193.513 02 | -45.7 | -59.8 |
| TS₂(15→16) | -193.341 78 | -193.333 30 | -61.1 | -74.4 |
| | -193.521 14 | -193.512 89 | -45.8 | -59.4 |

^a G2++ energies are shown in bold font, and G3 energies are in italic font. ^b Experimental value, taken from ref 43, is given in parentheses. ^c Experimental value, taken from ref 44, is given in parentheses.

TABLE 5: G2++ and G3 Total Energies^a (E_0), Enthalpies (H_{298}), and Standard Heats of Formation at 0 K (ΔH_f°) and 298 K (ΔH_f°) of the Species Involved in the Fragmentation Reaction of $(\text{CH}_3)_3\text{CO}^-$

| species | E_0 (hartrees) | H_{298} (hartrees) | ΔH_f° (kJ mol ⁻¹) | ΔH_f° (kJ mol ⁻¹) |
|------------------|---------------------|-------------------------|---|---|
| 17 | -232.632 38 | -232.624 99 | -246.9 | -271.8 |
| | -232.858 94 | -232.851 60 | -236.6 | -261.7 |
| | | | | (-275 ± 12) ^b |
| | | | | (-277 ± 9) ^c |
| 18 | -232.583 53 | -232.573 39 | -118.6 | -136.4 |
| | -232.808 70 | -232.799 08 | -104.7 | -123.8 |
| 19a + 19b | -232.637 04 | -232.627 23 | | |
| | -232.862 92 | -232.853 34 | | |
| TS(17→18) | -232.576 81 | -232.567 37 | -101.0 | -120.6 |
| | -232.801 39 | -232.791 98 | -85.5 | -105.1 |
| TS(18→19) | -232.584 01 | -232.574 63 | -119.9 | -139.6 |
| | -232.808 62 | -232.799 91 | -104.5 | -126.0 |

^a G2++ energies are shown in bold font, and G3 energies are in italic font. ^b Experimental value, taken from ref 43, is given in parentheses. ^c Experimental value, taken from ref 44, is given in parentheses.

developed within the complex provide an *entropy well* in which the system tends to linger.¹⁷ The potential energy surface (PES) of this *entropy-well* environ should be rather flat so that the lingering fragments can freely rotate relative to each other. Hence, such a complex would at most sit in a shallow potential energy well. Chemical engagement would not take place until the fragments properly orient relative to each other.²² It is generally accepted that a species will be considered as an INC

only if its lifetime from the point of covalent bond breaking to the point of overcoming long-range electrostatic forces is long enough that a chemical reaction other than dissociation has time to occur. From entropy (density of states) consideration, INCs are stable entities and have now achieved wide acceptance as viable intermediates in unimolecular dissociations of many types of ions.^{17,22,23,29}

Since the fragments of an INC show reactivities similar to those expected for the isolated species,^{23,30} it is not unreasonable to expect that the character of the INC or the INC-like TS for reaction 2a, for example, is dominated by either the IMC [$\text{H}^- \cdots \text{CH}_3\text{CHO}$] or ion-radical complex (IRC) [$\text{H} \cdots \text{CH}_3\text{CHO}^-$] state if the reaction is INC-mediated. One may therefore infer the nature of an INC-mediated reaction by comparing the energetics of its two limiting (heterolytic and homolytic) pathways.³⁰ The stabilization energy of an INC relative to its separated fragments with a nonpolar neutral is ca. 20–25 kJ mol⁻¹.³¹ Stabilization energies in the range of 42–80 kJ mol⁻¹ are common in INCs containing a polar neutral.^{23,32} The critical energies (assuming no reverse barriers) for the formation of the two limiting states (e.g., [$\text{H}^- \cdots \text{CH}_3\text{CHO}$] and [$\text{H} \cdots \text{CH}_3\text{CHO}^-$]) of the complex can then be easily estimated from their stabilization energies (relative to their corresponding separated fragments) and the ΔH_{f0} values for the direct homolytic ($\text{CH}_3\text{CH}_2\text{O}^- \rightarrow \text{H} + \text{CH}_3\text{CHO}^-$) and heterolytic ($\text{CH}_3\text{CH}_2\text{O}^- \rightarrow \text{H}^- + \text{CH}_3\text{CHO}$) dissociations. The relative stability of the two limiting states should be the dominant factor in determining whether the INC-mediated reaction occurs by a heterolytic or homolytic mechanism. Based on the results obtained from this simple ion-dipole model, we infer that the INCs involved in the eliminations studied in this work are IMCs rather than IRCs.

In this work, we did not carry out calculations of INCs formed from the final product pair prior to dissociation. When considering the possible intermediacy of INCs in unimolecular dissociations, a distinction must be made between a process in which the incipient product pair form a stable complex prior to dissociation, and a process which involved INCs as intermediates before the last chemical step.³³

Initial Bond Cleavage of Alkoxide Anions. There are two possible initiation steps for the elimination of H₂ or CH₄ from a simple alkoxide anion. It can start with either a homolytic or a heterolytic bond dissociation. In Table 1, it is seen that all heterolytic dissociations require less energy than the homolytic counterparts. In other words, heterolytic bond cleavage is favored over homolytic bond cleavage in the decompositions of alkoxide anions: the reaction should start with a heterolytic bond cleavage to form a ketone and a hydride ion or a carbanion rather than a homolytic bond cleavage producing a ketonic anion and a hydrogen atom or an alkyl radical.

Dissociation of Alkoxide Anions. In this section, we will discuss the anionic decomposition mechanisms of each alkoxide anion studied in this work.

Dissociation of CH₃O⁻ (I). There is only one elimination pathway for this anion, namely, the 1,1-elimination of H₂. It can be either concerted or stepwise. If it occurs by a concerted mechanism, it must be a highly asynchronous one^{34,35} since the synchronous and symmetrical stretching of the two C–H bonds should be symmetry forbidden. In agreement with Sheldon and Bowie's HF/6-311++G results,⁶ we found no such concerted and asynchronous pathway for reaction 1 at the MP2(Full)/6-31++G(d) level. The symmetry-forbidden pathway is a very high-energy process⁶ and is not a plausible mechanism for the occurrence of reaction 1.

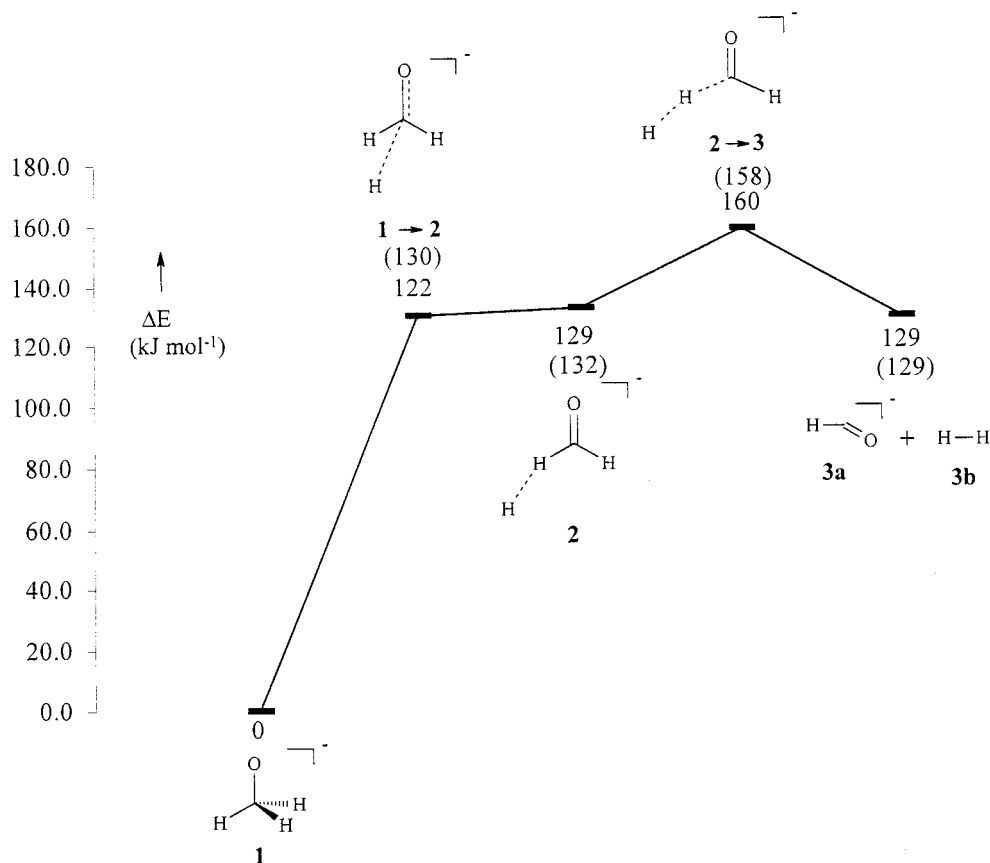
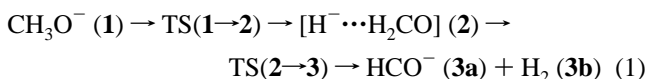


Figure 1. G2++ energy profiles of the dissociation for CH_3O^- (**1**). The G3 relative energies are given in parentheses.

On the MP2(Full)/6-31++G(d) PES, reaction 1 occurs by a stepwise mechanism:



However, on both the G2++ and G3 PESs, the minimum energy path (MEP) of reaction 1 appears to be a single-step pathway. From Figure 1 one may notice that $\text{TS}(\mathbf{1} \rightarrow \mathbf{2})$ is lower in energy than **2** by 7 kJ mol^{-1} at the G2++ level. Such an anomaly that a TS is slightly lower in energy than the local minimum to which it connects has been discussed previously.³⁶ Nevertheless, the deviation is somewhat too large and it suggests that optimization of the structure of $\text{TS}(\mathbf{1} \rightarrow \mathbf{2})$ at the MP2(Full)/6-31++G(d) level is not adequate enough. We recalculated the G2++ energies of $\text{TS}(\mathbf{1} \rightarrow \mathbf{2})$ and **2** based on their MP2(Full)/6-31++G(d,p) optimized structures and found that the former is now 3 kJ mol^{-1} lower in energy than the latter. With thermal and entropy corrections, their free energy difference at 298 K is essentially zero. Thus, initial formation of $[\text{H}^- \cdots \text{H}_2\text{CO}]$ from **1** proceeds essentially without or with a very small reverse barrier. In other words, the IMC is energetically unstable. Once it is formed its fragments readily undergo association reaction to form **1**. Though an IMC is not necessary to correspond to a local minimum,²⁹ it may sit in an *entropy well*¹⁷ and is *entropy stable* and its lifetime is long enough to await chemical engagement. The MEP of reaction 1 is so asynchronous that two distinct elementary processes can be clearly discerned: initial hydride anion elimination resulting the formation of $[\text{H}^- \cdots \text{H}_2\text{CO}]$, followed by proton abstraction within the complex. Reaction 1 proceeds by a stepwise mechanism. It has been questioned whether any reaction can be truly concerted.³⁴ The

barrier to the first step is 129 kJ mol^{-1} , and the barrier to the proton-transfer step within the complex is 31 kJ mol^{-1} .

This reaction was studied both experimentally and computationally by Bowie and co-workers.⁶ Their results are in qualitative agreement with our G2++ (or G3) data, even though there are significant quantitative differences between them. Specifically, at the HF/6-311++G level, Bowie et al. obtained the following relative energies (in kJ mol^{-1}) for the species involved in reaction 1: **1** (0), $\text{TS}(\mathbf{1} \rightarrow \mathbf{2})$ (142), **2** (126), $\text{TS}(\mathbf{2} \rightarrow \mathbf{3})$ (335), **3a+3b** (177). In other words, their overall barrier is more than twice that of the G2++ (or G3) counterpart. It is noted their HF/6-311++G structure⁶ of $\text{TS}(\mathbf{2} \rightarrow \mathbf{3})$ looks like a three-fragment complex structure $[\text{H} \cdots \text{HCO} \cdots \text{H}]^-$, and upon checking, we found that it is not a true local TS structure at the HF/6-311++G level. Furthermore, their IMC **2** has a symmetric structure with C_{2v} symmetry, instead of the unsymmetric geometry we obtained at the MP2(Full)/6-31G(d) and MP2(Full)/6-31++G(d) levels. It appears that the structure of **2** depends on whether the chosen basis set has polarization functions on the non-hydrogen atoms.

Large primary isotope effect (7.5) observed in reaction 1 was assigned to be due to the first step.⁶ The assignment of Bowie et al.⁶ was based on the calculated primary isotope effect (0.9) for the proton-transfer step. The calculation⁶ was based on the three-fragment complex structure which is a questionable TS for the proton-transfer step as mentioned in the previous paragraph. One should note that the program BEBOVIB IV³⁷ which was used for their calculation of isotope effect gives information which is critically dependent on TS geometries.⁹ As can be seen from Figure 5, the bridging $\text{C} \cdots \text{H}$ bond of $\text{TS}(\mathbf{2} \rightarrow \mathbf{3})$ is severely extended (1.463 Å). We rationalize that there should be a significant primary isotope effect manifested by the proton-transfer step since strong primary isotope effects have

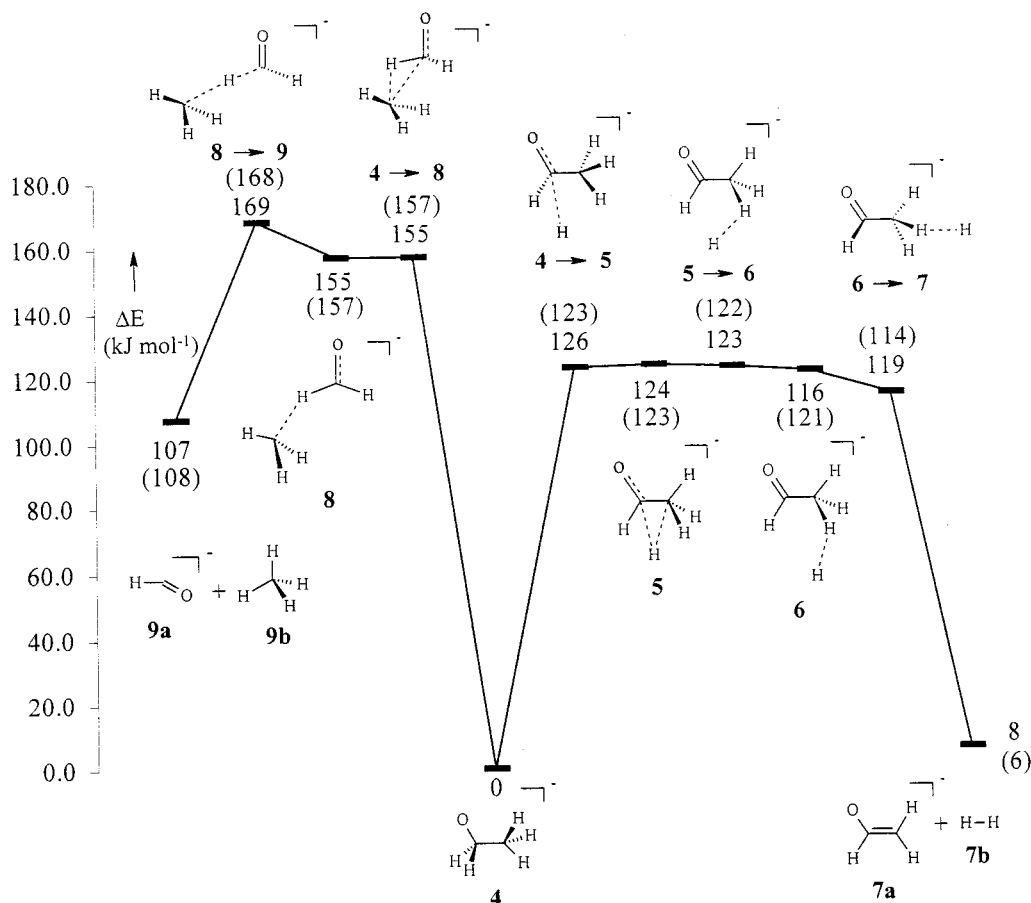
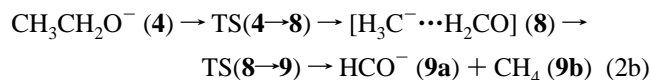
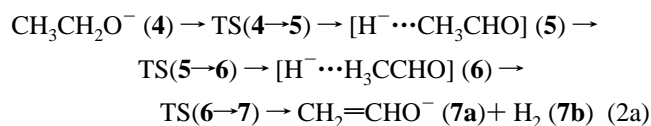


Figure 2. G2++ energy profiles of the dissociation for CH₃CH₂O⁻ (4). The G3 relative energies are given in parentheses.

been attributed to the TS for H transfer being higher in energy than that for cleavage to form the complex.³⁸

Previously we investigated loss of H₂ from 4, reaction 2a, at the G2++ level.¹⁴ The overall energy barrier (126 kJ mol⁻¹)¹⁴ to this reaction, which is also the energy barrier to the first step, is ca. 34 kJ mol⁻¹ less than that of reaction 1. This is in line with the observation⁶ that loss of H₂ from 1 is several orders of magnitude less probable than from 4. The unusually large energy barrier (ca. 31 kJ mol⁻¹) to the proton-transfer step within [H⁻⋯H₂CO], as compared to those found for other INC-mediated reactions investigated in this work and our previous studies,^{14,30,39} suggests that this step is also rate determining.

Dissociations of CH₃CH₂O⁻ (4). There are two elimination pathways to be studied, the 1,2-elimination of H₂, and 1,1-elimination of CH₄:



We now consider the loss of H₂ via IMC [H⁻⋯*c*-CH₂CH₂O], i.e., 4 → [H⁻⋯*c*-CH₂CH₂O] → H₂ + C₂H₃O⁻ (*c*-CH₂CHO⁻ or CH₂=CHO⁻). We found that the formation of the complex would be too energetic. Using the experimental Δ*H*_{f298} values⁴⁰ of 4, H⁻, H₂CO, CH₃CHO, and *c*-CH₂CH₂O as well as the stabilization energies^{23,31,32} of the INCs involved, it may be concluded that [H⁻⋯*c*-CH₂CH₂O] is higher in energy than

[H⁻⋯CH₃CHO] and [H₃C⁻⋯H₂CO] by ca. 118 and 69 kJ mol⁻¹, respectively. Obviously, this reaction channel is energetically noncompetitive to reactions 2a and 2b. Experimentally, fragmentation of the CH₃CD₂O⁻ anion resulted in elimination of HD only, excluding the 1,1-elimination mechanism.² In general, ethylene oxides are much higher in energy than their corresponding ketonic isomers.⁴⁰ We conclude that eliminations involving IMCs containing ethylene oxide or its substituted analogues are not energetically competitive to the reactions studied in this work. Studies of their reaction pathways are therefore not carried out.

It is noted that, in the G3 calculations of reaction 2a, the structures of species TS(4→5), 5, TS(5→6), 6, and TS(6→7) were optimized at the MP2(Full)/6-31++G(d) level since only TS(4→5), but not TS(5→6) and TS(6→7), was located at the MP2(Full)/6-31G(d) level. Also, the G2++ results for these two reactions are taken directly from ref 14. From Figure 2, it is seen that the 1,2-elimination of H₂ also starts with hydride ion elimination, followed by proton abstraction on the neighboring methyl group by this anion. On the other hand, the 1,1-elimination of CH₄ starts with dissociation of a methyl carbanion, followed by proton abstraction on the carbonyl carbon by the carbanion.

The G2++ PES for reaction 2a is atypical of a stepwise reaction pathway: initial formation of intermediate 6 via TS(4→5) which becomes the TS connecting 4 and 6, followed by proton transfer via TS(6→7). The barrier to the first step is 126 kJ mol⁻¹ and that to the second step is 3 kJ mol⁻¹. The TS(6→7) is lower in energy than TS(4→5) by 7 kJ mol⁻¹. Thus the first step is rate determining. That TS(6→7) has some proton-bridged character (the bridging C–H bond is 1.262 Å) as can

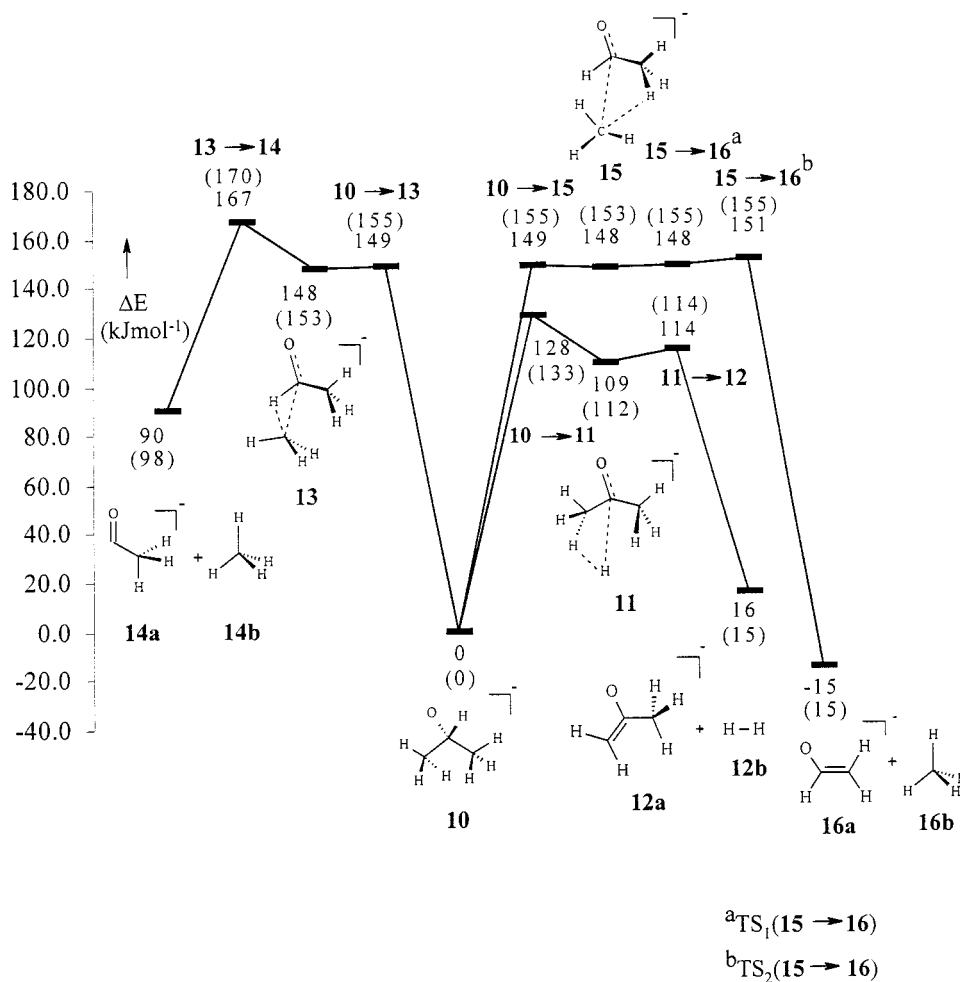


Figure 3. G2++ energy profiles of the dissociation for $(\text{CH}_3)_2\text{CHO}^-$ (**10**). The G3 relative energies are given in parentheses.

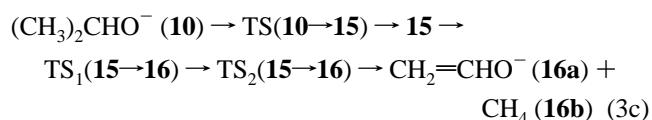
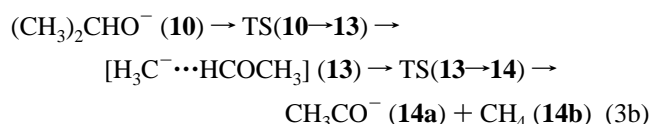
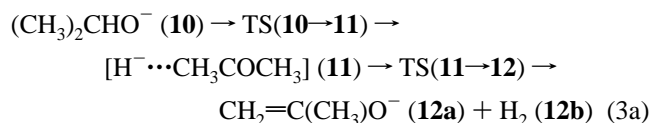
be seen from Figure 5 suggests the proton-transfer step may have a small primary isotope effect. A large primary isotope effect for this step would require a significant lengthening of the bridging C–H bond in the TS structure. This proton-transfer process would proceed through a highly asymmetric TS (in terms of the proton-bridged structure $[\text{C}\cdots\text{H}\cdots\text{H}]^-$) due to the large exothermicity (ca. 110 kJ mol^{-1}) of this step and therefore should exhibit a small primary isotope effect.⁴¹ The observed primary isotopic effect is $1.6\text{--}2.0$.^{9,12}

The G3 MEP of reaction 2a essentially has an energy barrier of 123 kJ mol^{-1} over which the complex spans a wide spectrum of IMC-like structures (e.g., TS(4→5), 5, TS(5→6), and 6). The small energy barrier (3 kJ mol^{-1}) to the proton-transfer process that appears on the G2++ PES vanishes at the G3 level which is based on MP2(Full)/6-31G(d) structures. It is known⁴² that use of diffuse and polarization functions centered on the H atom is significant in obtaining accurate energy of the hydride anion (H^-). Their effects on structures of IMCs consisting of a H^- fragment cannot be ignored. Obviously, the structures of $[\text{H}^- \cdots \text{CH}_3\text{CHO}]$ optimized at the MP2(Full)/6-31G(d) level are somewhat inferior to those obtained at the MP2(Full)/6-31++G(d) level. The single-barrier feature of the G3 PES is an artifact of using the MP2(Full)/6-31G(d) structures of $[\text{H}^- \cdots \text{CH}_3\text{CHO}]$. The importance of the use of polarization functions on the H atoms of $[\text{H}^- \cdots \text{H}_2\text{CO}]$ has been illustrated in the case of reaction 1.

The G2++ PES of reaction 2b is similar to that of reaction 1. Both are 1,1-elimination and have similar overall barrier height (160 kJ mol^{-1} for reaction 1 and 169 kJ mol^{-1} for

reaction 2b). The energy barrier to the initial C–C bond cleavage leading to the formation of **8** is 155 kJ mol^{-1} . This process proceeds without a reverse barrier. The energy barrier to the proton transfer within the complex $[\text{CH}_3^- \cdots \text{H}_2\text{CO}]$ is 14 kJ mol^{-1} . Based on these results, we rationalize that 1,1-elimination of H_2 from **4** would have a similar overall energy barrier (ca. 160 kJ mol^{-1}) if it ever occurs. Thus, 1,2- H_2 elimination is energetically favored over the 1,1-eliminations for **4**. This result agrees with those of the experiments: CAD^{2,9} and IRMP¹¹ studies on the ethoxide anion show that **4** undergoes 1,2-elimination of H_2 exclusively and no 1,1-elimination^{2,9} of H_2 occurs.

*Dissociations of $(\text{CH}_3)_2\text{CHO}^-$ (**10**).* There are three elimination pathways to be studied:



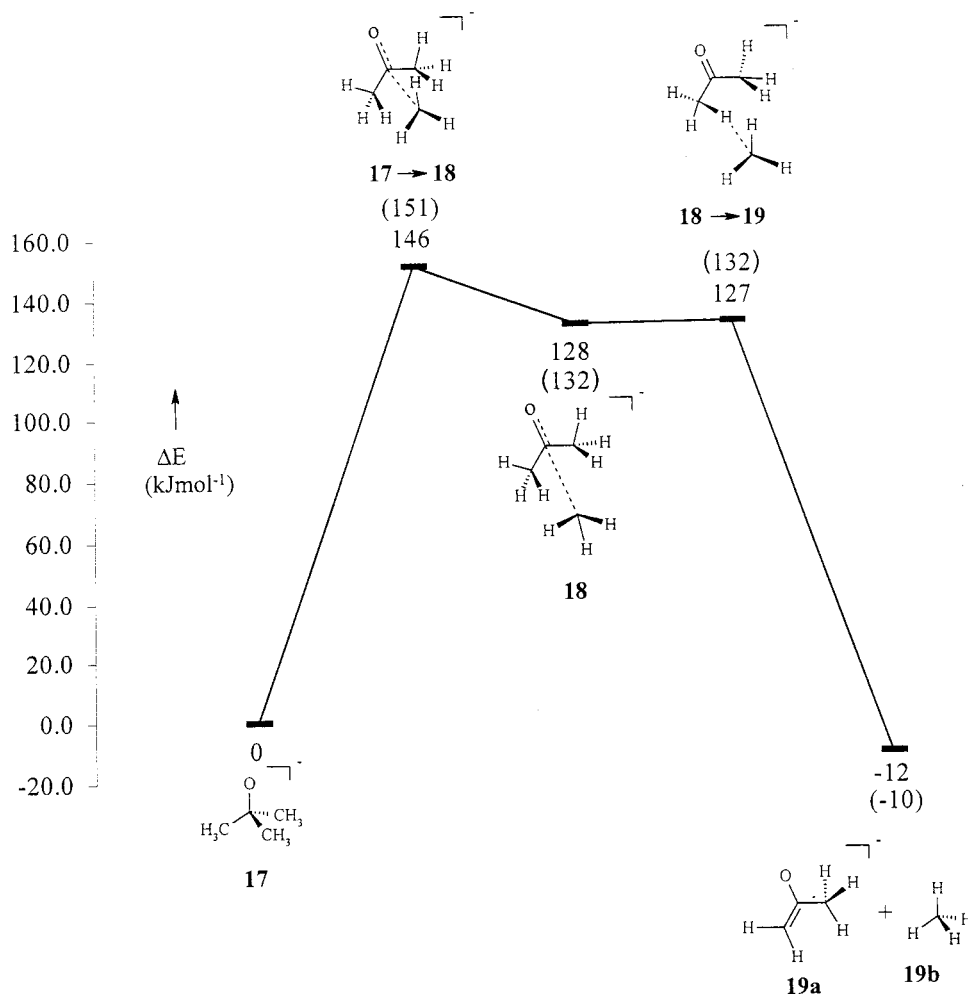


Figure 4. G2++ energy profiles of the dissociation for $(\text{CH}_3)_3\text{CO}^-$ (**17**). The G3 relative energies are given in parentheses.

The G2++ barriers for reaction 3a are 128 (first step) and 5 (second step) kJ mol^{-1} , similar to those for reaction 2a. The TS(**11**→**12**) has some proton-bridged character; however, the bridging C–H bond (1.290 Å) is still quite intact. Thus a small primary isotope effect would be manifested in the proton-transfer step as in the case of reaction 2a. This is in line with the measured value (2.0).⁹

Both the 1,1-elimination (reaction 3b) and 1,2-elimination (reaction 3c) of CH_4 start with the dissociation of methyl carbanion, followed by proton abstraction on the carbonyl and methyl carbon, respectively. The energy barriers to the first steps of reactions 3b and 3c are essentially the same, ca. 149 kJ mol^{-1} . However, the energy barrier to the proton-transfer step in reaction 3b is ca. 16 kJ mol^{-1} higher than that in reaction 3c. In addition, **16a** is lower in energy than **14a** by 105 kJ mol^{-1} . Hence, reaction 3c is thermodynamically and kinetically more favorable than reaction 3b.

Among reactions 3a, 3b, and 3c, the first one has the lowest critical energy. In other words, H_2 elimination is again energetically favored over CH_4 eliminations for **10**. This is consistent with the CAD result² that at the lowest collision energies elimination of H_2 is the dominant fragmentation reaction. This indicates that this reaction has the lower critical reaction energy and will be the channel observed when threshold reactions are probed by multiphoton activation. Indeed, Brauman and co-workers^{7,11} have reported that the infrared multiphoton photodissociation of **10** results in elimination of H_2 only. The rapid rise in importance of the 1,2-elimination of CH_4 , reaction 3c,

with increasing collision energy suggests that the critical energy for 1,2- CH_4 elimination should be slightly greater than that for H_2 elimination and there may be entropy effects which favor CH_4 elimination.² The calculated overall energy barrier to reaction 3c is ca. 23 kJ mol^{-1} higher than that to reaction 3a, in line with the conclusion inferred from the experimental result.²

While Mercer and Harrison² observed elimination of CD_4 and HD from $(\text{CD}_3)_2\text{CHO}^-$, Bowie et al.⁹ reported that CD_3H , CH_3D , and CH_4 were also eliminated from $(\text{CD}_3)_2\text{CHO}^-$, $(\text{CH}_3)_2\text{CDO}^-$, and $\text{CH}_3(\text{CD}_3)\text{CHO}^-$, respectively, reactions consistent with a 1,1-elimination. Energetically, reaction 3b is competitive to reaction 3c since the overall energy barrier of the former is only 16 kJ mol^{-1} higher than the latter. However, reaction 3b is 105 kJ mol^{-1} less exothermic than reaction 3c. The occurrence of reaction 3b is less probable than that of reaction 3c. 1,1-Elimination of H_2 from **1**, reaction 1, is plausible but is several orders of magnitude less probable than reaction 2a, a 1,2-elimination reaction. Our calculated results suggest that 1,1- CH_4 elimination is energetically plausible in fragmentation of **10**. However, it is less probable than 1,2-elimination of CH_4 and would be several orders of magnitude less probable than 1,2- H_2 loss from **10**. In conclusion, reactions 3a and 3c are the dominant channels in the fragmentation of **10**. If reaction 3b ever occurs, its elimination products will be in an insignificant amount.

*Dissociation of $(\text{CH}_3)_3\text{CO}^-$ (**17**).* There is only one pathway to be studied, the 1,2-elimination of CH_4 other than loss of H_2

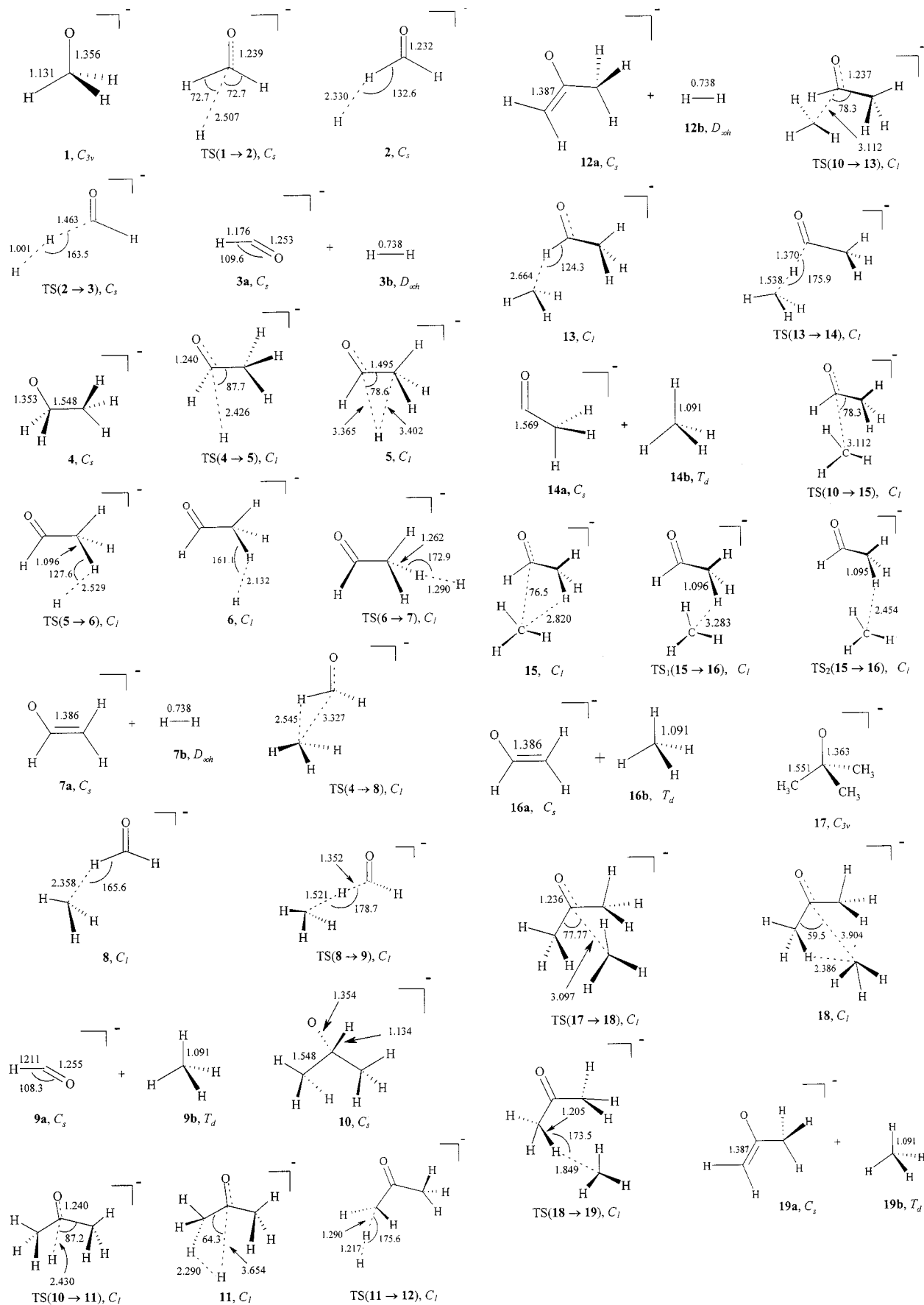
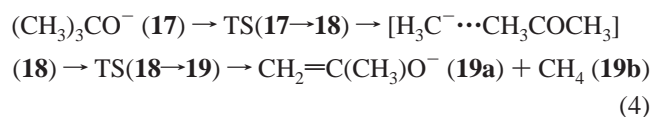


Figure 5. Optimized structures of all the species involved in the fragmentation reactions of the four alkoxide anions studied in this work. All the structures were optimized at the MP2(Full)/6-31++G(d) level.

via $[H\cdots c-CH_2OC(CH_3)_2]$:



From Figure 4, it is seen that the G2++ barrier for the elimination of CH_4 is 146 kJ mol^{-1} (the G3 result is quite similar). This barrier height is close to that (151 kJ mol^{-1}) of reaction 3c. This CH_4 dissociation involves the methyl carbanion elimination, followed by proton abstraction on the neighboring methyl group by this carbanion. There exists no energy barrier to the proton-transfer process. The structure of $TS(18 \rightarrow 19)$ is IMC-like, suggesting the primary isotope effect for the proton-transfer step would be small. The measured values^{9,12} range from 1.6 to 2.1.

In passing, it is noted that the calculated G2++/G3 heats of formation for the four alkoxide anions studied (**1**, **4**, **10**, and **17**) are in very good accord with the experimental data available in the literature. In particular, the excellent agreement between the G2++ and the experimental results is especially noticeable. Such an agreement should give credence to the other reported energies such as the energies and activation barriers of the reactions studied in this work.

Conclusions

The dissociation mechanisms of four simple alkoxide anions, CH_3O^- (**1**), $CH_3CH_2O^-$ (**4**), $(CH_3)_2CHO^-$ (**10**), and $(CH_3)_3CO^-$ (**17**), were studied by the ab initio G2++ and G3 methods. For each anion, the calculated heat of reaction for the heterolytic dissociation was found to be smaller than that of the homolytic one. This result shows that the decomposition reactions should start with heterolytic bond cleavage.

Based on our calculated results, it is concluded that the dissociation of these alkoxide anions should proceed via a stepwise mechanism: H_2 dissociation from an alkoxide anion starts with hydride anion elimination, followed by proton abstraction by the hydride anion. Similarly, CH_4 dissociation from an alkoxide anion starts with methyl carbanion elimination, followed by proton abstraction by the carbanion. Between the hydride/carbanion elimination and proton abstraction, an IMC intermediate is formed.

For the fragmentation pathways of (**4**) and of (**10**), 1,2- H_2 elimination has a lower energy barrier than 1,1- or 1,2- CH_4 eliminations. The overall energy barriers of 1,1-elimination reactions studied range from 160 to 170 kJ mol^{-1} . 1,2- H_2 eliminations have a barrier range of 126–128 kJ mol^{-1} and 1,2- CH_4 eliminations have a barrier height (146–151 kJ mol^{-1}) between those of 1,1- CH_4 and 1,2- H_2 eliminations. These results are in accord with the CAD^{2,9} and IRMP¹¹ studies of **4** that only H_2 elimination is observed. The calculated results are also in line with the low-energy CAD study² of **10** that 1,2- H_2 elimination is the dominant channel observed among its fragmentation pathways. Elimination of CH_4 from **10** increases as collision energy increases.² It has two plausible pathways: 1,1- and 1,2-elimination mechanisms. Our calculated results suggest that the occurrence of the 1,2-elimination pathway should be dominant over the 1,1-elimination pathway, in accord with the experimental results² that CD_4 and HD are observed from CAD study of $(CD_3)_2CHO^-$.

In addition, the calculated G2++/G3 heats of formation of these alkoxide anions, **1**, **4**, **10**, and **17**, are in excellent agreement with available experimental data. The use of the basis set 6-31G(d) may be inadequate in characterizing IMC structures

having a H^- fragment. Overall, the G3 results, which are based on MP2(Full)/6-31G(d) structures, are qualitatively comparable to the G2++ results although the PES landscape calculated at the G3 level for reaction 2a is qualitatively different from that obtained at the G2++ level.

If an alkoxide anion is represented by the general formula $(R^1)(R^2)(R^3)CO^-$, the anions studied in this work are the special cases with $R^1, R^2, R^3 = H$ or CH_3 . Currently under investigation are the anions with $R^1, R^2, R^3 = CH_3, C_2H_5$, or *i*-Pr. With these systems, steric effects as well as electronic effects will be the controlling factors for their decomposition reactions.

Acknowledgment. J.K.C.L. and W.K.L. are grateful to the Computer Services Centre of The Chinese University of Hong Kong for its generous allocation of computer time on the SGI Origin 2000 High-Performance Server.

References and Notes

- Hass, J. M.; Harrison, A. G. *Int. J. Mass Spectrom. Ion Processes* **1993**, *124*, 115.
- Mercer, R. S.; Harrison, A. G. *Can. J. Chem.* **1988**, *66*, 2947.
- Raftery, M. J.; Bowie, J. H.; Sheldon, J. C. *J. Chem. Soc., Perkin Trans. 2* **1988**, 563.
- Eichinger, P. C. H.; Bowie, J. H. *J. Chem. Soc., Perkin Trans. 2* **1988**, 497.
- Eichinger, P. C. H.; Bowie, J. H.; Blumenthal, T. *J. Org. Chem.* **1986**, *51*, 5078.
- Sheldon, J. C.; Bowie, J. H.; Lewis, D. E. *New J. Chem.* **1988**, *12*, 269.
- Tumas, W.; Foster, R. F.; Pellerite, M. J.; Brauman, J. I. *J. Am. Chem. Soc.* **1984**, *106*, 4053.
- Tumas, W.; Foster, R. F.; Pellerite, M. J.; Brauman, J. I. *J. Am. Chem. Soc.* **1983**, *105*, 7464.
- Hayes, R. N.; Sheldon, J. C.; Bowie, J. H.; Lewis, D. E. *Aust. J. Chem.* **1985**, *38*, 1197.
- Hayes, R. N.; Sheldon, J. C.; Bowie, J. H.; Lewis, D. E. *J. Chem. Soc., Chem. Commun.* **1984**, 1431.
- Tumas, W.; Foster, R. F.; Brauman, J. I. *J. Am. Chem. Soc.* **1988**, *110*, 2714.
- Tumas, W.; Foster, R. F.; Pellerite, M. J.; Brauman, J. I. *J. Am. Chem. Soc.* **1987**, *109*, 961.
- Mercer, R. S.; Harrison, A. G. *Org. Mass Spectrom.* **1987**, *22*, 710.
- Chiu, S.-W.; Lau, K.-C.; Li, W.-K. *J. Phys. Chem. A* **1999**, *103*, 6003.
- Mestres, J.; Duran, M.; Bertran, J.; Csizmadia, I. G. *J. Mol. Struct. (THEOCHEM)* **1995**, *358*, 229.
- Wiberg, K. B. *J. Am. Chem. Soc.* **1990**, *112*, 3379.
- McAdoo, D. *J. Mass Spectrom. Rev.* **1988**, *7*, 363.
- Frisch, M. J.; Trucks, G. W.; Schlegel, H. B.; Gill, P. M. W.; Johnson, B. J.; Robb, M. A.; Cheeseman, J. R.; Keith, T. A.; Petersson, G. A.; Montgomery, J. A.; Raghavachari, K.; Al-Laham, M. A.; Zarkewski, V. G.; Ortiz, J. V.; Foresman, J. B.; Cioslowski, J.; Stefanov, B. B.; Nanayakkara, A.; Challacombe, M.; Peng, C. Y.; Ayala, P. Y.; Chen, W.; Wong, M. W.; Andres, J. L.; Replogle, E. S.; Gomperts, R.; Martin, R. L.; Fox, D. J.; Binkley, J. S.; Defrees, D. J.; Baker, J.; Stewart, J. J. P.; Head-Gordon, M.; Gonzalez, C.; Pople, J. A. *GAUSSIAN 94*, Revision D4; Gaussian, Inc.: Pittsburgh, PA, 1995.
- Frisch, M. J.; Trucks, G. W.; Schlegel, H. B.; Scuseria, G. E.; Robb, M. A.; Cheeseman, J. R.; Zakrzewski, V. G.; Montgomery, J. A., Jr.; Stratmann, R. E.; Burant, J. C.; Dapprich, S.; Millam, J. M.; Daniels, A. D.; Kudin, K. N.; Strain, M. C.; Farkas, O.; Tomasi, J.; Barone, V.; Cossi, M.; Cammi, R.; Mennucci, B.; Pomelli, C.; Adamo, C.; Clifford, S.; Ochterski, J.; Petersson, G. A.; Ayala, P. Y.; Cui, Q.; Morokuma, K.; Malick, D. K.; Rabuck, A. D.; Raghavachari, K.; Foresman, J. B.; Cioslowski, J.; Ortiz, J. V.; Baboul, A. G.; Stefanov, B. B.; Liu, G.; Liashenko, A.; Piskorz, P.; Komaromi, I.; Gomperts, R.; Martin, R. L.; Fox, D. J.; Keith, T.; Al-Laham, M. A.; Peng, C. Y.; Nanayakkara, A.; Gonzalez, C.; Challacombe, M.; Gill, P. M. W.; Johnson, B.; Chen, W.; Wong, M. W.; Andres, J. L.; Gonzalez, C.; Head-Gordon, M.; Replogle, E. S.; Pople, J. A. *GAUSSIAN 98*, Revision A.7; Gaussian, Inc.: Pittsburgh, PA, 1998.
- Curtiss, L. A.; Raghavachari, K.; Redfern, P. C.; Redfern, V.; Pople, J. A. *J. Chem. Phys.* **1998**, *109*, 7764.
- Curtiss, L. A.; Raghavachari, K.; Trucks, G. W.; Pople, J. A. *J. Chem. Phys.* **1991**, *94*, 7221.
- Morton, T. H. *Org. Mass Spectrom.* **1992**, *27*, 353.
- Bowen, R. D. *Acc. Chem. Res.* **1991**, *24*, 364.

- (24) Moylan, C. R.; Brauman, J. I. *J. Am. Chem. Soc.* **1985**, *107*, 761.
- (25) Audier, H. E.; Bouchoux, G.; McMahon, T. B.; Milliet, A.; Vulpus, T. *Org. Mass Spectrom.* **1994**, *29*, 176.
- (26) Nguyen, M. T.; Bouchoux, G. *J. Phys. Chem.* **1996**, *100*, 2089.
- (27) Wang, D.; Squires, R. B. *Int. J. Mass Spectrom. Ion Processes Rev.* **1991**, *107*, 7.
- (28) Heinrich, N.; Louage, F.; Lifshitz, C.; Schwarz, H. *J. Am. Chem. Soc.* **1988**, *110*, 8183.
- (29) Chronister, E. L.; Morton, T. H. *J. Am. Chem. Soc.* **1990**, *112*, 133.
- (30) Chiu, S.-W.; Cheung, Y.-S.; Ma, N. L.; Li, W.-K.; Ng, C. Y. *J. Mol. Struct. (THEOCHEM)* **1999**, *468*, 21.
- (31) McAdoo, D. J.; Traeger, J. C.; Hudson, C. E.; Griffin, L. L. *J. Chem. Phys.* **1988**, *92*, 9524.
- (32) Kebarle, P. *Annu. Rev. Phys. Chem.* **1977**, *28*, 445.
- (33) Hammerum, I. S.; Hansen, M. M.; Audier, H. E. *Int. J. Mass Spectrom.* **1977**, *160*, 183.
- (34) Dewar, M. J. S. *J. Am. Chem. Soc.* **1984**, *106*, 209.
- (35) Gajewski, J. *Acc. Chem. Res.* **1980**, *13*, 142.
- (36) Cheung, Y.-S.; Li, W.-K.; Ng, C. Y. *J. Mol. Struct. (THEOCHEM)* **1995**, *339*, 25.
- (37) Sims, L. B.; Burton, B. W.; Lewis, D. W. *Quantum Chem. Prog. Exch.* **1977**, No. 337.
- (38) Hudson, C. E.; McAdoo, D. J. *Int. J. Mass Spectrom. Ion Processes* **1984**, *59*, 325.
- (39) Chiu, S.-W.; Lau, K.-C.; Li, W.-K.; Ma, N. L.; Cheung, Y.-S.; Ng, C. Y. *J. Mol. Struct. (THEOCHEM)* **1999**, *490*, 109.
- (40) *NIST Chemistry WebBook*; Mallard, W. G., Linstrom, P. J., Eds.; NIST Standard Reference Database Number 69, November 1998; National Institute of Standards and Technology: Gaithersburg, MD 20899 (<http://webbook.nist.gov>).
- (41) Melander, L.; Saunders, W. H. *Reactions of Isotopic Molecules*; Wiley: New York, 1980.
- (42) Li, W.-K. *J. Chem. Educ.* **1994**, *71*, 1094.
- (43) Lias, S. G.; Bartmess, J. E.; Liebman, J. F.; Holmes, J. L.; Levin, R. D.; Mallard, W. G. *J. Phys. Chem. Ref. Data* **1988**, *17* (Suppl.1).
- (44) Haas, M. J.; Harrison, A. G. *Int. J. Mass Spectrom. Ion. Processes* **1993**, *124*, 115.